

Search for Heavy Neutral Leptons with IceCube DeepCore

Dissertation

zur Erlangung des akademischen Grades
doctor rerum naturalium
(Dr. rer. nat.)

im Fach: Physik
Spezialisierung: Experimentalphysik

eingereicht an der
Mathematisch-Naturwissenschaftlichen Fakultät
der Humboldt-Universität zu Berlin

von

Leander Fischer M. Sc.
geboren am 24. Oktober 1992
in Heidelberg

Präsidentin der Humboldt-Universität zu Berlin
Prof. Dr. Julia von Blumenthal

Dekanin der Mathematisch-Naturwissenschaftlichen Fakultät
Prof. Dr. Caren Tischendorf

Copyright Notice

This book is released into the public domain using the CC-BY-4.0 code.

To view a copy of the CC-BY-4.0 code, visit:

<https://creativecommons.org/licenses/by/4.0/>

Colophon

This document was typeset with the help of KOMA-Script and L^AT_EX using the open-source kaobook template class.

The source code of this thesis is available at:

https://github.com/LeanderFischer/phd_thesis

Zusammenfassung

Zusammenfassung ...

Abstract

Abstract ...

Todo list

(Re-)write introduction for PhD thesis (just copy paste from M.Sc.).	1
cite Higgs	3
(Re-)write SM neutrino chapter for PhD thesis (just copy paste from M.Sc.).	3
Re-write/re-formulate this section (copied from HNL technote).	4
Produce similar styled plot for these limits	4
This section really needs to be re-written to motivate the search for HNLs from a more generic point of view (e.g. to explain neutrino masses)	5
This section definitely needs to be elaborated in a little more detail	6
Not adding information about the case where the neutrinos have Dirac or pseudo-Dirac masses	6
Plot is missing + for W and 0 for Z boson.	9
SB: It seems that you have some double counting of information here . I suggest to move some of the information in this "intro" paragraph to the appropriate subsections	10
Explain momenta and momentum transfer (p,q) in these figures.	11
(Re-)write BSM chapter for PhD thesis (just copy paste from M.Sc.).	11
SB: You could say why with an extra half-sentence.	12
SB: I don't think this is true - the normalization is known to 5% if you trust Anatoli/Juan Pablo. Please have a look at more recent publications on this topic.	12
SB: formatting/margins also I don't think you defined rho1,2	12
add information about the matter profile used	17
add information about the oscillation probability calculation and the software used for it	17
Should I adapt the total numbers to match the sum of the rounded individual parts?	17
add 3D expectation and/or S/sqrt(B) plots	18
Add fractions of the different particle types in the bins for benchmark mass/mixing (another table?) .	18
Do I want/need to include the description of the KDE muon estimation?	19
Add table with all systematic uncertainties used in this analysis (in the analysis chapter).	19
add final level effects of varying the axial mass parameters (or example of one)	19
add final level effects of varying the DIS parameter (or example of one)	19
Do I want additional plots for this (fit diff, LLH distr, minim. stats, param. fits)?	20
Add bin-wise TS distribution? Add 3D TS maps?	21
Re-make plot with x,y for horizontal set one plot!	25
Re-make plot with x, y, z for both cascades in one.	25
Re-arrange plots in a more sensible way.	25

Contents

Abstract	iii
Contents	vii
1 Introduction	1
2 Standard Model Neutrinos and Beyond	3
2.1 The Standard Model	3
2.1.1 Electroweak Symmetry Breaking	3
2.1.2 Fermion Masses	4
2.2 Evidence for Beyond Standard Model Physics	4
2.3 Heavy Neutral Leptons	4
2.3.1 A Solution to (some of) the Problems	4
2.3.2 The Minimal Standard Model Extension	5
2.3.3 Existing Constraints on Heavy Neutral Leptons	7
2.4 Atmospheric Neutrinos	8
2.4.1 Properties and Interactions	8
2.4.2 Mass Mechanisms	8
2.4.3 Oscillations	11
2.4.4 Heavy Neutral Lepton Production and Decay in IceCube DeepCore	13
3 Detecting Low Energetic Double Cascades	15
3.1 Reconstruction	15
3.1.1 Table-Based Minimum Likelihood Algorithms	15
3.1.2 Double Cascade Hypothesis	15
3.1.3 Modification to Low Energy Events	15
3.2 Cross Checks	15
3.2.1 Simplistic Sets	15
3.3 Performance	16
3.3.1 Energy/Decay Length Resolution	16
3.3.2 Double Cascade Classification	16
4 Search for an Excess of Heavy Neutral Lepton Events	17
4.1 Final Level Sample	17
4.1.1 Expected Rates/Events	17
4.1.2 Analysis Binning	18
4.2 Statistical Analysis	19
4.2.1 Low Energy Analysis Framework	19
4.2.2 Test Statistic	19
4.2.3 Systematic Uncertainties	19
4.3 Analysis Checks	19
4.3.1 Minimization Robustness	20
4.3.2 Ensemble Tests	20
4.4 Results	21
4.4.1 Best Fit Parameters	21
4.4.2 Upper Limits	21
4.4.3 Post-Fit Data/MC Agreement	21
4.4.4 Likelihood Coverage	21

APPENDIX	23
A Heavy Neutral Lepton Signal Simulation	25
A.1 Model Independent Simulation Distributions	25
A.2 Model Dependent Simulation Distributions	26
B Analysis Checks	27
B.1 Minimization Robustness	27
B.1.1 Ensemble Tests	27
Bibliography	29

List of Figures

2.1	Current $ U_{\tau 4}^2 - m_4$ limits	5
2.2	Feynman diagram of HNL up-scattering process	7
2.3	Feynman diagram of HNL decay	7
2.4	HNL branching ratios	8
2.5	HNL decay widths	8
2.6	Feynman diagrams of neutrino weak interactions	9
2.7	Total inclusive neutrino-nucleon cross-sections	10
2.8	Neutrino-nucleon deep inelastic scattering	11
2.9	Atmospheric neutrino fluxes	11
4.1	Asimov inject/recover test (0.6 GeV)	20
4.2	Pseudo-data trials TS distribution (0.6 GeV)	21
A.1	Simplified model independent simulation generation level distributions	25
A.2	Realistic model independent simulation generation level distributions	26
A.3	Model dependent simulation generation level distributions	26
B.1	Asimov inject/recover test (0.3 GeV, 1.0 GeV)	27
B.2	Pseudo-data trials TS distribution (0.3 GeV, 1.0 GeV)	27

List of Tables

4.1	Final level background event/rate expectation	17
4.2	Final level signal event/rate expectation	18
4.3	Analysis binning	18
4.4	Staged minimization routine settings	20

notes for the introduction

- unexplained origin of neutrino masses
- novel neutrino mass

The neutrino was postulated by Wolfgang Pauli [1] in 1930 to explain the continuous energy spectrum of electrons originating from beta decay. Cowan and Reines confirmed this prediction of a light, neutral particle in 1956 when they discovered the electron neutrino using inverse beta decay [2]. Two additional neutrino flavors were found in the following years, and with the discovery of the muon neutrino in 1962 [3] and the tau neutrino in 2001 [4], the current theory of neutrinos in the standard model (SM) was established.

Although neutrinos were first believed to be massless, experimental evidence showing the existence of mixed neutrino states started to appear in the 1960s [5]. Mixing between different physical representations of neutrinos is proof for differences in their masses. The resulting phenomenon of neutrino oscillations can be incorporated into the standard model by extending it to include massive neutrinos. How massive they are and how strong is the mixing between neutrino states has to be obtained from measurement. Today there are a variety of precision oscillation experiments using solar, reactor and atmospheric neutrinos to tighten the constraints on the neutrino oscillation parameters. IceCube is one of those leading experiments probing the oscillation theory with atmospheric neutrinos.

The IceCube Neutrino Observatory [6] was constructed between 2004 and 2010 at the geographic South Pole. It is the first cubic kilometer Cherenkov neutrino detector and consists of 5160 optical sensors attached to 86 strings, drilled down to a maximum depth of ~ 2500 m into the Antarctic ice. Neutrinos are detected by the Cherenkov light that is emitted by secondary particles produced in neutrino-nucleon scattering interactions in the ice. With DeepCore, a more densely instrumented sub-array of IceCube, the neutrino detection energy threshold can be lowered to approximately 5 GeV.

At these energies, the similarity in event signatures poses difficulties in identifying different neutrino flavor interactions. Muon neutrino charged-current interactions produce light tracks as opposed to charged-current interactions of electron and tau neutrinos as well as neutral-current interactions of all neutrinos that produce light cascades. The sparse instrumentation of IceCube makes it more challenging to separate track- and cascade-like events. In this thesis, a novel method to distinguish those two event types is developed. In contrast to previously used univariate separation techniques, the multivariate machine learning method applied here maximizes the use of information from the detector response. Through the use of a Gradient Tree Boosting algorithm the separation of events in track and cascade is improved. As a result of

(Re-)write introduction for PhD thesis (just copy paste from M.Sc.).

[1]: Pauli (1978), "Dear radioactive ladies and gentlemen"

[2]: Cowan et al. (1956), "Detection of the Free Neutrino: a Confirmation"

[3]: Danby et al. (1962), "Observation of High-Energy Neutrino Reactions and the Existence of Two Kinds of Neutrinos"

[4]: Kodama et al. (2001), "Observation of tau neutrino interactions"

[5]: Davis et al. (1972), *Proceedings of the Neutrino '72 Europhysics Conference*

[6]: Aartsen et al. (2017), "The IceCube Neutrino Observatory: instrumentation and online systems"

the improved separation, the uncertainty to the atmospheric neutrino oscillation parameters Δm_{32}^2 and θ_{23} is significantly reduced.

This thesis is structured as follows.

Standard Model Neutrinos and Beyond

2

some history on the SM?

Yang-Mills theory (relativistic quantum field theory) EM, weak, strong interactions

all matter is made up of fermions, which are divided into quarks and leptons leptons are excitations of fermion fiels (Dirac type) bosons describe the interactions between the fermions that have to fulfil overall symmetry of the theory

completion in the mid-1970s gives very accurate predictions of Weak, Strong, and EM interactions also explains mechanisms giving quarks and leptons their mass - the Higgs mechanism - and predicts the existence of the Higgs boson which was discovered in 2012 at the LHC

it cannot explain some observations/phenomena like gravity (incompatibility with general relativity) or cosmological observations (dark matter, dark energy, matter-antimatter asymmetry)

and it does not predict neutrinos to have mass, which is experimentally proven by neutrino oscillations, so some extensions to the SM is needed in order to explain them

This chapter introduces the basic properties of neutrinos, their place in the Standard Model of particle physics (SM) and their peculiarities following the description of [7, 8].

2.1	The Standard Model . . .	3
2.2	Evidence for Beyond Standard Model Physics .	4
2.3	Heavy Neutral Leptons . .	4
2.4	Atmospheric Neutrinos .	8

cite Higgs

(Re-)write SM neutrino chapter for PhD thesis (just copy paste from M.Sc.).

[7]: Giunti et al. (2007), *Fundamentals of Neutrino Physics and Astrophysics*
[8]: Schwartz (2013), *Quantum Field Theory and the Standard Model*

2.1 The Standard Model

2.1.1 Electroweak Symmetry Breaking

$SU(3)_C \times SU(2)_L \times U(1)_Y$ local gauge symmetry, with conserved quantities C , color, L , left-handed chirality, and Y , weak hypercharge

Through spontaneous symmetry breaking of $SU(2)_L \times U(1)_Y$ the gauge bosons of the weak interaction (W and Z bosons) acquire their masses.

Without the broken symmetry, they would be massless, like the exchange bosons of the $SU(3)_C$ symmetry (gluons).

the Lagrangian of the Higgs field is given by

$$\mathcal{L}_{Higgs} = (D_\mu \Phi^\dagger)(D^\mu \Phi) - \lambda \left(\Phi^\dagger \Phi - \frac{v^2}{2} \right)^2, \quad (2.1)$$

with parameters λ and v . λ is assumed to be positive.

$$\Phi = \begin{pmatrix} \Phi^+ \\ \Phi^0 \end{pmatrix}, \quad (2.2)$$

non-zero *vacuum expectation value* (*vev*) at minimum of potential at $\Phi^\dagger \Phi = \frac{v^2}{2}$

vacuum is electrically neutral, so it can only come from a neutral component of the Higgs doublet as

$$\Phi_{\text{vev}} = \frac{1}{\sqrt{2}} \begin{pmatrix} 0 \\ v \end{pmatrix}. \quad (2.3)$$

2.1.2 Fermion Masses

mass term for charged fermions with spin-1/2 is given by

$$\mathcal{L}_{\text{Dirac}} = m(\bar{\Psi}_R \Psi_L - \bar{\Psi}_L \Psi_R), \quad (2.4)$$

a product of left- and right-handed Weyl spinors $\Psi_{L/R}$.

which is not invariant under $\text{SU}(2)_L \times \text{U}(1)_Y$ gauge transformations. Adding a Yukawa term coupling the fermion fields to the Higgs field recovers the invariance and gives the fermions their masses.

$$\mathcal{L}_{\text{Yukawa}} = -y \bar{L}_L \Phi e_R + \text{h.c.}, \quad (2.5)$$

y is the Yukawa coupling constant and \bar{L}_L is the $\text{SU}(2)_L$ doublet

with the vev this results in the mass term for the charged leptons and down-type quarks of $-m_e(\bar{e}_L e_R + \bar{e}_R e_L)$ with $m_e = \frac{yv}{\sqrt{2}}$.

2.2 Evidence for Beyond Standard Model Physics

- hierarchy problem
- strong-CP
- Matter-antimatter asymmetry
- Dark matter
- Neutrino masses

2.3 Heavy Neutral Leptons

2.3.1 A Solution to (some of) the Problems

Re-write/re-formulate this section (copied from HNL technote).

[9]: Yanagida (1980), "Horizontal Symmetry and Masses of Neutrinos"

Produce similar styled plot for these limits

[15]: Coloma et al. (2017), "Double-Cascade Events from New Physics in Icecube"

Extensions to the Standard Model (SM) that add *Heavy Neutral Leptons* (HNLs) provide a good explanation for the origin of neutrino masses through different seesaw mechanisms [9]. While the mixing with $\nu_{e/\mu}$ is strongly constrained ($|U_{\alpha 4}^2| \lesssim 10^{-5} - 10^{-8}$, $\alpha = e, \mu$), the mixing with ν_τ is much harder to probe due to the difficulty of producing and detecting ν_τ . Figure 2.1 shows the current limits on the τ -sterile mixing space for HNL masses between 0.1 GeV-10 GeV. As was first pointed out in [15], the atmospheric neutrino flux observed in IceCube offers a way to constrain the neutrino-HNL mixing parameters. By using the large

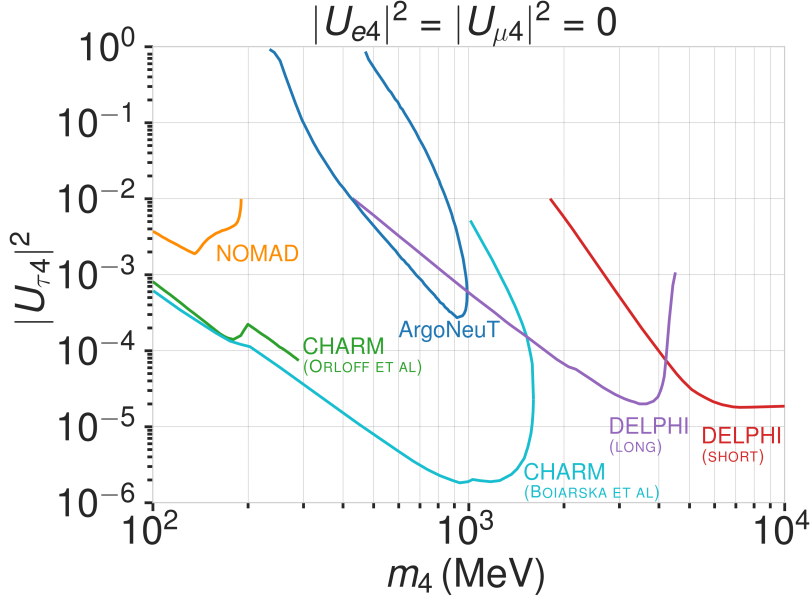


Figure 2.1: Current $|U_{\tau 4}|^2 - m_4$ limits from NOMAD [10], ArgoNeuT [11], CHARM [12, 13], and DELPHI [14].

fraction of atmospheric ν_μ events that oscillate into ν_τ before they reach the detector, the less constrained τ -sterile mixing space can be explored. In this document, we present the methodology and strategy of a search for HNLs with IceCube DeepCore. These additional *right-handed* (RH) neutrinos can be included in the Standard Model (SM) by extending the PMNS matrix to at least a 3x4 matrix as

$$\begin{pmatrix} \nu_e \\ \nu_\mu \\ \nu_\tau \end{pmatrix} = \begin{pmatrix} U_{e1} & U_{e2} & U_{e3} & U_{e4} \\ U_{\mu 1} & U_{\mu 2} & U_{\mu 3} & U_{\mu 4} \\ U_{\tau 1} & U_{\tau 2} & U_{\tau 3} & U_{\tau 4} \end{pmatrix} \begin{pmatrix} \nu_1 \\ \nu_2 \\ \nu_3 \\ \nu_4 \end{pmatrix}, \quad (2.6)$$

where the components with index 4 define the mixing between the flavor states and the fourth sterile mass state, respectively. Note here that this is not a theoretically fully consistent picture, but rather the phenomenologically minimal model to be tested by this analysis. This can hopefully be put into the larger context of several fully consistent models, later. Due to the singlet nature of the RH neutrinos, they only interact weakly, inheriting these interactions from their *left-handed* (LH) neutrino counterparts via mixing. This mixing of the HNLs with the electron, muon, and tau neutrinos can be probed and constrained as a function of the HNL mass by searching for their production and decay. In [15, 16] this search is mainly motivated through two experimental arguments. Secondly, IceCube is ideally placed to explore the yet unconstrained $|U_{\tau 4}|^2 - m_4$ phase-space that is not easily accessible by accelerator-based experiments.

2.3.2 The Minimal Standard Model Extension

In order to probe the τ -sterile mixing parameter, it is required to look at interactions involving τ neutrinos. However, most neutrinos produced in cosmic ray interactions with the atmosphere are ν_e or ν_μ . Therefore, we need these neutrinos to oscillate to the τ flavor before reaching the

[15]: Coloma et al. (2017), “Double-Cascade Events from New Physics in Icecube”

[16]: Coloma (2019), “Icecube/DeepCore tests for novel explanations of the Mini-BooNE anomaly”

This section really needs to be re-written to motivate the search for HNLs from a more generic point of view (e.g. to explain neutrino masses)

detector. For this to happen at the considered energies a traveled distance of the order of the earth diameter is necessary. This is why our signal is mostly up-going and passing through the whole earth.

This section definitely needs to be elaborated in a little more detail

[17]: Coloma et al. (2021), "GeV-scale neutrinos: interactions with mesons and DUNE sensitivity"

To explain the signature we can observe in IceCube we first have to revisit the weak interactions that the HNL inherits from its LH counterpart through mixing. We will be following the derivation in [17]. Extending the SM by n additional RH neutrinos, ν_i ($i = 3 + n$), leads to the mass Lagrangian

$$\mathcal{L}_\nu^{\text{mass}} \supset - \sum_{\alpha=e,\mu,\tau} \sum_{i=4}^{3+n} Y_{\nu,\alpha i} \bar{L}_{L,\alpha} \tilde{\phi} \nu_i - \frac{1}{2} \sum_{i=4}^{3+n} M_i \bar{\nu}_i \nu_i^c + \text{h.c.}, \quad (2.7)$$

in a basis where the Majorana mass terms are diagonal. $Y_{\nu,\alpha i}$ are the Yukawa couplings to the lepton doublets and M the Majorana masses for the heavy singlets. $L_{L,\alpha}$ stands for the SM LH lepton doublet of flavor α while ϕ is the Higgs field, and $\tilde{\phi} = i\sigma_2 \phi^*$ and $\nu_i^c \equiv C \bar{\nu}_i^t$, with $C = i\gamma_0 \gamma_2$ in the Weyl representation. The full neutrino mass matrix with the Higgs vacuum expectation value $v/\sqrt{2}$ reads

Not adding information about the case where the neutrinos have Dirac or pseudo-Dirac masses

$$\mathcal{M} = \begin{pmatrix} 0_{3 \times 3} & Y_\nu v/\sqrt{2} \\ Y_\nu^t v/\sqrt{2} & M \end{pmatrix}, \quad (2.8)$$

and can be diagonalized by a $(3 + n) \times (3 + n)$ full unitary rotation U , that itself leads to neutrino masses upon diagonalization, additionally manifesting the mixing between active neutrinos and heavy states. The resulting model consists of 3 light SM neutrino mass eigenstates ν_i ($i = 1, 2, 3$) and n heavier states, as introduced above. The flavor states will now consist of a combination of light and heavy states

$$\nu_\alpha = \sum_{i=1}^{3+n} U_{\alpha i} \nu_i, \quad (2.9)$$

and the leptonic part of the EW Lagrangian can be written as

$$\begin{aligned} \mathcal{L}_{\text{EW}}^\ell = & \frac{g}{\sqrt{2}} W_\mu^+ \sum_\alpha \sum_i U_{\alpha i}^* \bar{\nu}_i \gamma^\mu P_L \ell_\alpha + \frac{g}{4c_w} Z_\mu \\ & \times \left\{ \sum_{i,j} C_{ij} \bar{\nu}_i \gamma^\mu P_L \nu_j + \sum_\alpha \bar{\ell}_\alpha \gamma^\mu [2s_w^2 P_R - (1 - 2s_w^2) P_L] \ell_\alpha \right\} + \text{h.c.}, \end{aligned}$$

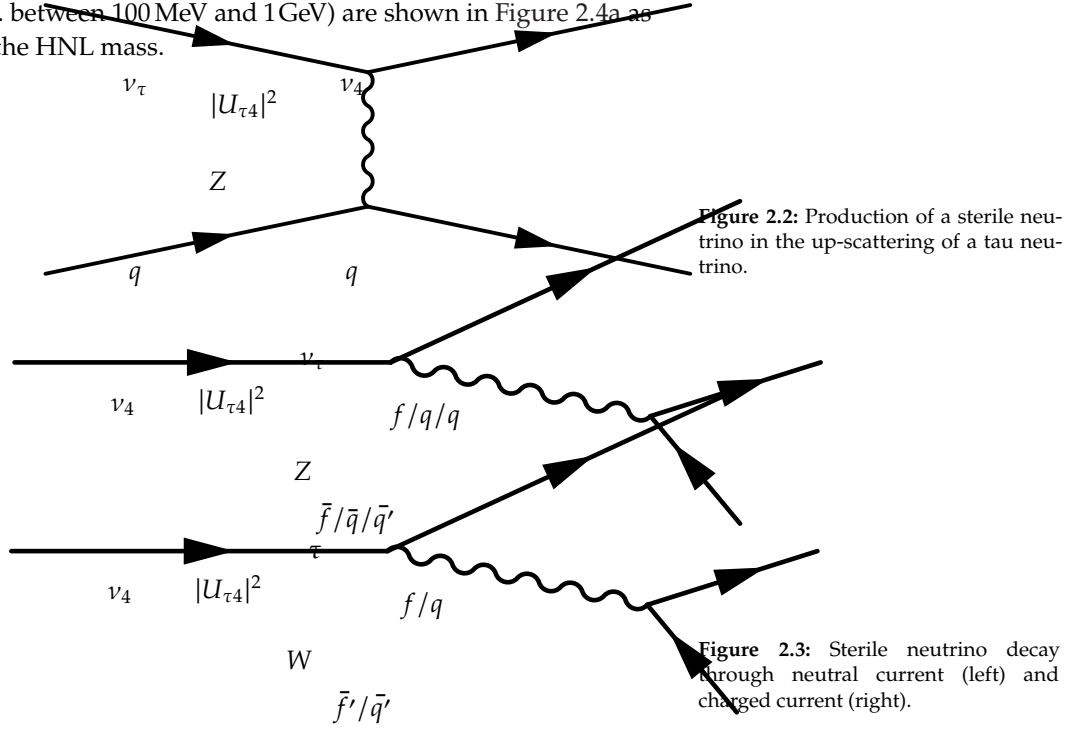
where $c_w \equiv \cos \theta_w$, $s_w \equiv \sin \theta_w$, and θ_w the SM weak mixing angle. P_L and P_R are the left and right projectors, respectively, while

$$C_{ij} \equiv \sum_\alpha U_{\alpha i}^* U_{\alpha j}. \quad (2.10)$$

The indices now sum over all $(3 + n)$ flavor and mass states.

Based on this formulation and assuming that only the mixing with the tau sector is open ($|U_{\alpha 4}^2| = 0$, $\alpha = e, \mu$), the relevant production diagram of the HNL can be drawn as shown in Figure 2.2. Alongside the fourth heavy mass state, a Hadronic cascade is produced. The heavy mass state will travel for some distance (dependent on mass and mixing) before it decays. The subsequent decay processes are depicted in Figure 2.3. It can be a CC or NC decay and both leptonic and mesonic modes are possible

(dependent on the mass). This will produce a tau or a tau neutrino and another cascade that can be Electromagnetic or Hadronic. The branching ratios corresponding to the decay modes of the HNL for the mass range of interest (i.e. between 100 MeV and 1 GeV) are shown in Figure 2.4a as a function of the HNL mass.



2.3.3 Existing Constraints on Heavy Neutral Leptons

xx constraints

yy constraints

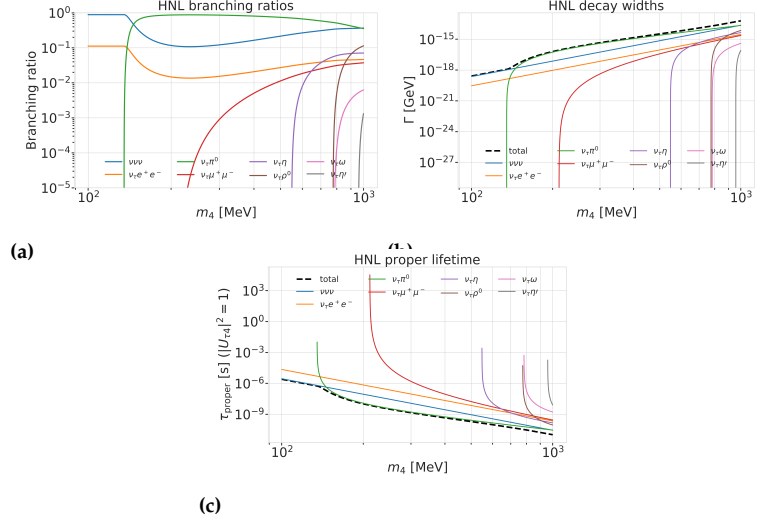


Figure 2.4: Branching ratios, decay widths, and proper lifetime of the HNL within the mass range considered, calculated based on the results from [17].

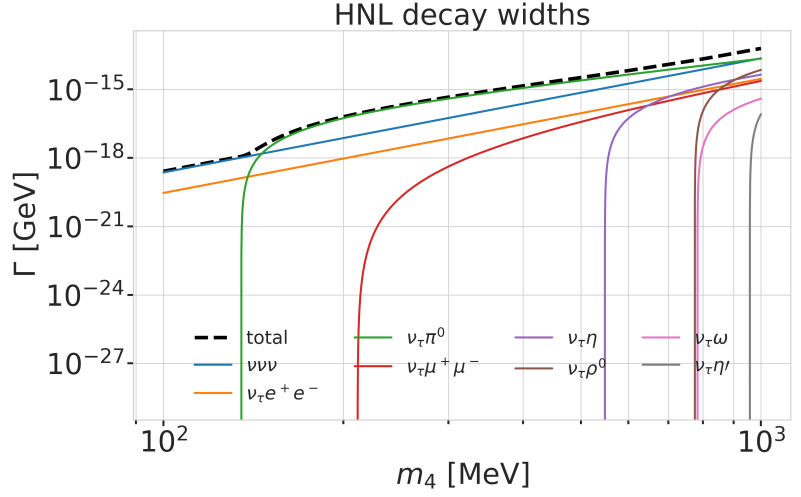


Figure 2.5: Decay widths of the HNL within the mass range considered, calculated based on the results from [17]. Given the existing constraints on $|U_{e4}|^2$ and $|U_{\mu4}|^2$, we consider that the corresponding decay modes are negligible.

2.4 Atmospheric Neutrinos

2.4.1 Properties and Interactions

2.4.2 Mass Mechanisms

Dirac

Majorana

See-Saw Variants

Radiative Neutrino Masses

Quantum Numbers

Active Neutrino Flavors

Weak Interactions after Symmetry-Breaking

The neutrino is an elementary particle in the SM [18]. It belongs to the class of leptons, which itself is a subclass of elementary fermions (spin $\frac{1}{2}$ particles). The fermions - six quarks and six leptons - form the matter content of the universe. Quarks take part in all three interaction types (forces) of the SM: strong, weak, and electromagnetic (EM) [19]. The charged leptons - electron, muon, and tau - are subject to the weak and the EM interaction. Neutrinos carry neither electric charge nor color charge and therefore only take part in weak interactions. There are three distinct neutrino flavors - electron neutrinos, muon neutrinos and tau neutrinos (ν_e , ν_μ , and ν_τ) [20] - each corresponding to their charged lepton counterparts.

In the SM, weak interactions are mediated by the three massive bosons W^+ , W^- , and Z^0 [18]. The large boson masses ($m_W \sim 80 \text{ GeV}$, $m_Z \sim 90 \text{ GeV}$) result in a short range of the force of about $10 \times 10^{-18} \text{ m}$. Weak interactions carried by W^\pm bosons are called charged-current (CC) interactions, because charge is transferred between the interacting particles. In CC interactions, a neutrino is converted into its corresponding charged lepton or vice versa. Neutral current (NC) interactions are those mediated by Z^0 bosons. Here no charge is transferred. The Feynman diagrams for CC and NC interactions are shown in Figure 2.6.

Although neutrinos are massless in the SM, we know today that they do have a small mass. The observed phenomenon of neutrino oscillations (see Section 2.4.3) is based on the fact that there is a mass difference between the three neutrino mass eigenstates. From neutrino oscillation measurements the absolute mass scale cannot be determined, since they only depend on the mass differences, but there are upper limits on the sum of all neutrino masses from cosmological observations. These upper limits are typically between 0.3 and 1.3 eV [20].

Neutrino-Lepton Scattering

Neutrino Interactions with Nuclei

To describe the neutrino detection principle of IceCube explained in Chapter ?? we need to understand the weak interaction processes that occur at the energies relevant for this work 10 GeV-100 GeV. The cross-sections are dominated by the following neutrino-nucleon interactions: quasi-elastic scattering (QE), resonant scattering (RES), and deep inelastic scattering (DIS). The relative importance of the different processes depends on energy as can be seen in Figure 2.7.

At energies below 5 GeV, QE and RES occur and the neutrinos interact with approximately point-like protons and neutrons. The cross-sections of these processes are not linear in energy and the transition region to higher energies is poorly understood. At higher energies, the interactions are dominated solely by DIS which has a linear dependence on energy

[18]: Thomson (2013), *Modern particle physics*

[19]: Glashow (1961), "Partial-symmetries of weak interactions"

[20]: Tanabashi et al. (2018), "Review of Particle Physics"

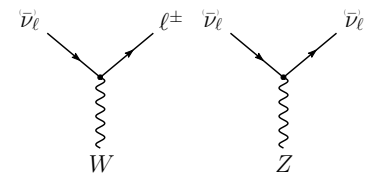


Figure 2.6: Feynman diagrams of charged-current (left) and neutral-current (right) neutrino weak interactions, taken from [21].

Plot is missing + for W and 0 for Z boson.

[18]: Thomson (2013), *Modern particle physics*

[20]: Tanabashi et al. (2018), "Review of Particle Physics"

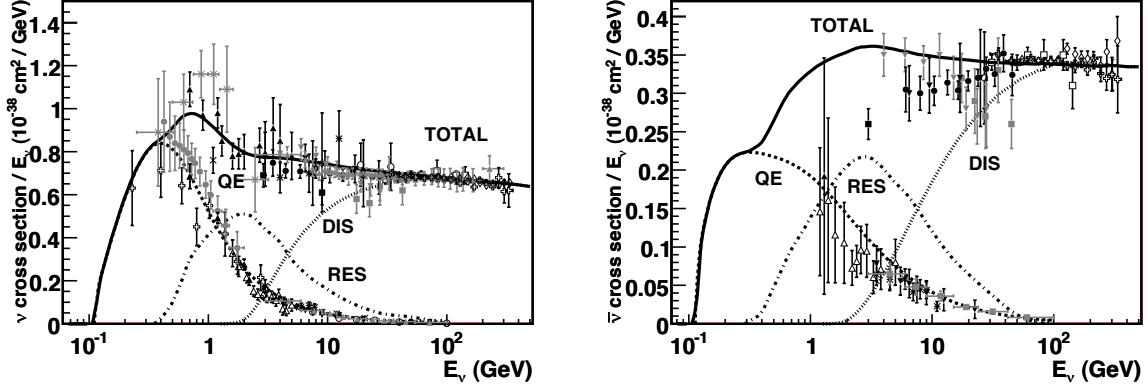


Figure 2.7: Total neutrino(left) and antineutrino(right) per nucleon cross-section divided by neutrino energy plotted against energy. The three main scattering processes quasi-elastic scattering (QE), resonant scattering (RES), and deep-inelastic scattering (DIS) are depicted. Taken from [22].

SB: It seems that you have some double counting of information here . I suggest to move some of the information in this "intro" paragraph to the appropriate subsections

above ~ 20 GeV. For a given neutrino energy, it is possible to predict the cross-section in this region. Here neutrinos interact with a single quark, breaking apart the nucleus and producing a shower of relativistic secondary particles. Neutrino DIS is the primary detection channel of IceCube. From Figure 2.7 it can be seen that the interaction cross-sections are very small of the order of 10^{-38} cm^2 . Because of the small interaction cross-section, very large volume detectors are required to capture a sufficiently large sample of neutrinos to use for precision studies of their properties. For example, the interaction length of a neutrino with $E_\nu = 10 \text{ GeV}$ is of $\mathcal{O}(10^{10} \text{ km})$.

Quasi-elastic scattering (QE) with nucleons is the main process below 1 GeV. Protons are converted to neutrons in antineutrino interactions and vice-versa for neutrino interactions. Additionally, a charged lepton corresponding to the neutrino/antineutrino flavor is produced.

Resonant scattering (RES) describes the process of a neutrino scattering off a nucleon producing an excited state of the nucleon in addition to a charged lepton. RES is the leading process at $1.5 \times 10^{-5} \text{ GeV}$ for neutrinos and $1.5 \times 10^{-8} \text{ GeV}$ for antineutrinos.

Deep inelastic scattering (DIS) occurs if a neutrino carries sufficient energy to resolve the underlying structure of the nucleon and interacts with one of the composing quarks. DIS is the dominant process above 10 GeV. The nucleon breaks up and a lepton accompanied by a set of hadronic final states is produced. Whether the lepton is the charged lepton corresponding to the interacting neutrino type, or the neutrino itself depends on the type of DIS interaction. DIS happens via CC as in

$$\begin{aligned} \nu_l + N &\rightarrow l^- + X, \\ \bar{\nu}_l + N &\rightarrow l^+ + X, \end{aligned} \quad (2.11)$$

or NC interactions as

$$\nu_l + N \rightarrow \nu_l + X. \quad (2.12)$$

Here, X stands for any set of final state hadrons and N for the nucleon. The Feynman diagrams for the processes in Equation 2.11 and Equation 2.12 are shown in Figure 2.8.

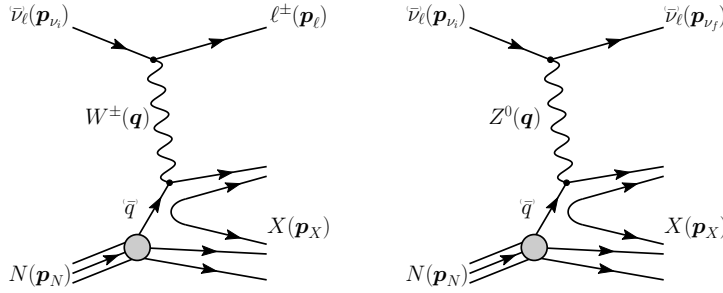


Figure 2.8: Feynman diagrams for deep inelastic scattering of a neutrino with a nucleon via charged-current (left) and neutral current (right) interactions. Taken from [21].

2.4.3 Oscillations

The flux of neutrinos used for this work exclusively comes from the Earth's atmosphere. When highly relativistic cosmic rays (protons and heavier nuclei [20]) interact in the upper atmosphere they produce a shower of particles. Neutrinos emerge from the decays of charged pions and kaons (π and K mesons) present in these showers. For energies below 100 GeV, the leading contribution comes from the pion decay chain

$$\begin{aligned}\pi^\pm &\rightarrow \mu^\pm + \nu_\mu(\bar{\nu}_\mu), \\ \mu^\pm &\rightarrow e^\pm + \bar{\nu}_\mu(\nu_\mu) + \nu_e(\bar{\nu}_e).\end{aligned}\quad (2.13)$$

The muons that also originate from this process are considered the main background source for IceCube. The left part of Figure 2.9 shows the atmospheric neutrino flux for the very broad energy spectrum in which they are produced. The flux expectations are calculated in the energy range of 100 MeV to 10 TeV for the South Pole [23], where the IceCube detector is located. From Equation 2.13 the ratio between muon and electron neutrinos can be inferred to be $N_{\nu_\mu} : N_{\nu_e} \approx 2 : 1$. This is only the case at muon energies below 1 GeV, where all muons decay in flight. For higher energies, muons can reach earth before decaying increasing the ratio to approximately 10:1 at around 100 GeV as shown in the right part of Figure 2.9. Additionally, kaon decays start to contribute which also increases the number of muons and muon neutrinos.

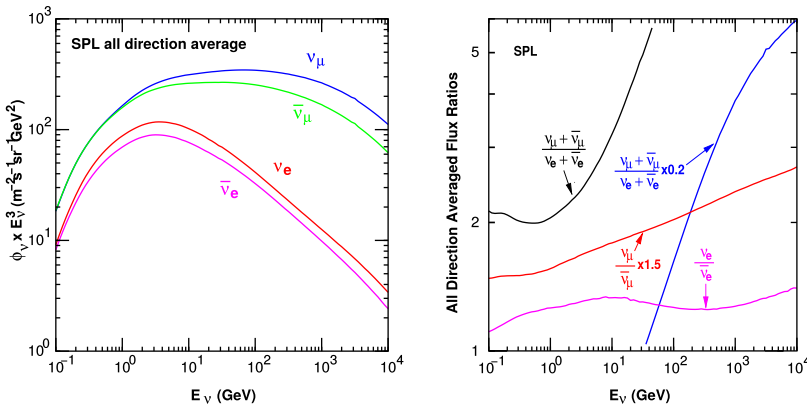


Figure 2.9: Atmospheric neutrino fluxes of the different flavors as a function of energy (left) and ratios between muon and electron neutrinos as well as ratios between neutrinos and antineutrinos for both flavors (right). Calculations are done for the geographic South Pole. Taken from [23].

In cosmic ray interactions, charged mesons or tau particles can also be

Explain momenta and momentum transfer (p, q) in these figures.

(Re-)write BSM chapter for PhD thesis (just copy paste from M.Sc.).

[20]: Tanabashi et al. (2018), "Review of Particle Physics"

[23]: Honda et al. (2015), "Atmospheric neutrino flux calculation using the NRLMSISE-00 atmospheric model"

[24]: Fedynitch et al. (2015), "Calculation of conventional and prompt lepton fluxes at very high energy"

SB: You could say why with an extra half-sentence.

[25]: Honda et al. (2007), "Calculation of atmospheric neutrino flux using the interaction model calibrated with atmospheric muon data"

SB: I don't think this is true - the normalization is known to 5% if you trust Anatoli/Juan Pablo. Please have a look at more recent publications on this topic.

[26]: Bilenky et al. (1978), "Lepton mixing and neutrino oscillations"

[20]: Tanabashi et al. (2018), "Review of Particle Physics"

[20]: Tanabashi et al. (2018), "Review of Particle Physics"

SB: formatting/margins also I don't think you defined rho1,2

produced, which leads to the formation of tau neutrinos. However, at the energy range considered for this work, the resulting tau neutrino flux is negligible as compared to the muon neutrino flux [24] and is not taken into account. It should be stated here that there is a rather large uncertainty on the normalization of the atmospheric neutrino flux on the order of 20-30 % [25] in the energy region of interest. This is mainly due to uncertainties in the primary cosmic ray spectrum and modeling of the hadronic interactions.

There are two ways to describe neutrino wave functions based on their Hamiltonian eigenvalues [26], as mass eigenstates or as flavor eigenstates. When applying a plane wave approach to explain the propagation of neutrinos in vacuum, their mass eigenstates evolve as

$$|v_k(t)\rangle = e^{-iE_k t/\hbar} |v_k\rangle, \quad (2.14)$$

where $E_k = \sqrt{\vec{p}^2 c^2 + m_k^2 c^4}$ is the energy of the mass eigenstate $|v_k\rangle$, with momentum \vec{p} and mass m_k . Alternatively, they can be described in terms of their flavor eigenstates, which relate the neutrinos to the charged leptons they interact with in weak CC interactions. The flavor eigenstates are ν_e, ν_μ , and ν_τ , whereas the mass eigenstates are called ν_1, ν_2 , and ν_3 in the standard three-neutrino model. To understand the propagation of distinct neutrino flavors in time we need to relate the flavor eigenstates to the mass eigenstates. For massive neutrinos, each flavor eigenstate is a superposition of mass eigenstates [20]

$$|\nu_\alpha\rangle = \sum_k U_{\alpha k}^* |\nu_k\rangle, \quad (2.15)$$

where $|\nu_\alpha\rangle$ are the weak flavor states with $\alpha = e, \mu, \tau$ and $|\nu_k\rangle$ the mass states with $k = 1, 2, 3$. $U_{\alpha k}$ is the Pontecorvo-Maki-Nakagawa-Sakata (PMNS) matrix defining the mixing between mass and flavor eigenstates. The mixing matrix can be parameterized as [20]

$$U = \begin{pmatrix} 1 & 0 & 0 \\ 0 & c_{23} & s_{23} \\ 0 & -s_{23} & c_{23} \end{pmatrix} \begin{pmatrix} c_{13} & 0 & s_{13}e^{-i\delta_{CP}} \\ 0 & 1 & 0 \\ -s_{13}e^{i\delta_{CP}} & 0 & c_{13} \end{pmatrix} \begin{pmatrix} c_{12} & s_{12} & 0 \\ -s_{12} & c_{12} & 0 \\ 0 & 0 & 1 \end{pmatrix} \text{diag}(e^{i\rho_1}, e^{i\rho_2}, 1), \quad (2.16)$$

where $c_{ij} = \cos \theta_{ij}$ and $s_{ij} = \sin \theta_{ij}$ are cosine and sine of the mixing angle θ_{ij} , that defines the strength of the mixing between the mass eigenstates i and j and δ_{CP} is the neutrino CP-violating phase. Nonzero, non-equal neutrino masses and the neutrino mixing relation in Equation 2.15 lead to the observed phenomenon of neutrino oscillations. Oscillation means that a neutrino changes from its initial flavor to another flavor and back after traveling a certain distance. A produced flavor eigenstate $|\nu_\alpha\rangle$ propagates through space as a superposition of mass eigenstates. To find the probability that the initial flavor state $|\nu_\alpha\rangle$ ends up as the final flavor state $|\nu_\beta\rangle$ after the time t we calculate

$$P_{\nu_\alpha \rightarrow \nu_\beta}(t) = |\langle \nu_\beta | \nu_\alpha(t) \rangle|^2, \quad (2.17)$$

where P is the probability calculated by applying Fermi's Golden Rule [27]. Fermi's Golden Rule explains the transition rate from one energy eigenstate to another depending on the strength of the coupling between the two. The strength of the coupling is described by the square of the

[27]: Dirac (1927), "The Quantum Theory of the Emission and Absorption of Radiation"

matrix element. Using the unitarity of the mixing matrix $U^{-1} = U^\dagger$ to reverse the relation Equation 2.15 and then time evolve the mass eigenstates with Equation 2.14 we get the time evolution of the flavor state $|\nu_\alpha(t)\rangle$. Inserting this result into Equation 2.17 yields

$$P_{\nu_\alpha \rightarrow \nu_\beta}(t) = \sum_{j,k} U_{\beta j}^* U_{\alpha j} U_{\beta k} U_{\alpha k}^* e^{-i(E_k - E_j)t/\hbar}, \quad (2.18)$$

where the indices j and k run over the mass eigenstates. For small neutrino masses compared to their kinetic energy, we can approximate the energy as

$$E_k \approx E + \frac{c^4 m_k^2}{2E} \longrightarrow E_k - E_j \approx \frac{c^4 \Delta m_{kj}^2}{2E}, \quad (2.19)$$

where $\Delta m_{kj}^2 = m_k^2 - m_j^2$ is the mass-squared splitting between states k and j . If we now replace the time in Equation 2.18 by the distance traveled by the relativistic neutrinos $t \approx L/c$ we get

$$\begin{aligned} P_{\nu_\alpha \rightarrow \nu_\beta}(L) = & \delta_{\alpha\beta} - 4 \sum_{j>k} \text{Re}(U_{\beta j}^* U_{\alpha j} U_{\beta k} U_{\alpha k}^*) \sin^2\left(\frac{c^3 \Delta m_{kj}^2}{4E\hbar} L\right) \\ & + 2 \sum_{j>k} \text{Im}(U_{\beta j}^* U_{\alpha j} U_{\beta k} U_{\alpha k}^*) \sin^2\left(\frac{c^3 \Delta m_{kj}^2}{4E\hbar} L\right), \end{aligned} \quad (2.20)$$

which is referred to as the survival probability if $\alpha = \beta$ and the transition probability if $\alpha \neq \beta$. The probability in Equation 2.20 is only nonzero if there are neutrino mass eigenstates with masses greater than zero. Additionally, there must be a mass-squared difference Δm^2 and nonzero mixing between the states. Since we assumed propagation in vacuum in Equation 2.14, the transition and survival probabilities correspond to vacuum mixing.

2.4.4 Heavy Neutral Lepton Production and Decay in IceCube DeepCore

Detecting Low Energetic Double Cascades

3

3.1 Reconstruction

3.1 Reconstruction 15

3.1.1 Table-Based Minimum Likelihood Algorithms

3.2 Cross Checks 15

3.1.2 Double Cascade Hypothesis

3.3 Performance 16

3.1.3 Modification to Low Energy Events

3.2 Cross Checks

3.2.1 Simplistic Sets

After generation the events are processed with standard Photon, Detector, L1, and L2 processing and then Taupede+MuMillipede is run on top of the L2 files. Multiple versions with different parameters were produced, some with the OscNext baseline parameters, some without detector noise (in Det level) and some with h2-50cm holeice model, to match the holeice model that was used to generate the photonics tables.

BrightDom Cleaning To investigate the effect of the BrightDom cleaning cut the 194601 set without detector noise (and baseline hole ice model) is used. The BrightDom cleaning is needed to stop a few DOMs with many photon hits to drive the reconstruction because this leads to large biases in the energy estimations. Historically, the BrightDom cleaning was removing all DOMs that had a charge larger than 10 times the mean charge. After quickly checking some charge distributions and how the mean behaves it was clear that the cut should better be defined based on a metric that is less affected by outliers, like the median. Figure ?? shows where the mean and the median are located for an example event. The cut was re-defined to use the median instead of the mean and 10% of the simulation were processed with Taupede using 30x and 100x the median as BrightDom cutoff. Figure ?? shows where these values fall for the same example event.

As a quick check of the performance of both cuts the decay length resolution/bias and the resolutions/biases of all energies were checked. The reconstructed decay length is almost not affected by applying this cut, which is as expected, because it is mostly dependent on the arrival time of the photons. The effect on the reconstructed energy is much stronger, where a looser cut (100x) shows a significantly larger bias than the tighter cut at (30x). Even though this was not a highly sophisticated optimization of the BrightDom cut, an improvement was achieved by changing from mean to median and selecting the tighter cut (of the two tested). It's hard to tell how this would perform for high energy events, but I'm quite certain that a definition based on the median would be more reliable than on the mean.

3.3 Performance

3.3.1 Energy/Decay Length Resolution

3.3.2 Double Cascade Classification

Search for an Excess of Heavy Neutral Lepton Events

4

The measurement performed in this thesis is the search for an excess of HNL events in the 10 years of IceCube DeepCore data. In principle the two physics parameters to be probed are the mass of the HNL, m_4 , and the mixing between the fourth heavy mass state and the SM τ sector, $|U_{\tau 4}|^2$. Since the mass itself influences the production and decay kinematics of the event and the accessible decay modes, individual mass sets were produced as described in Section ???. The mass slightly influences the energy distribution, while the mixing both changes the overall scale of the HNL events and the shape in energy and PID. IceCube DeepCore is suited to measure the excess which appears around and below 20 GeV, due to its production from the atmospheric tau neutrinos, although a reduced lower energy threshold could improve the analysis. The measurement will be performed for the three mass sets individually, while the mixing is the parameter that can be varied continuously and will be measured in the fit.

4.1	Final Level Sample	17
4.2	Statistical Analysis	19
4.3	Analysis Checks	19
4.4	Results	21

4.1 Final Level Sample

The final level sample of this analysis always consists of the neutrino and muon MC introduced in Section ?? and one of the three HNL samples explained in Section ??. All of those simulation sets and the 10 years of IceCube DeepCore data are processed through the full processing and event selection chain described in Section ?? leading to the final level sample. Since applying the last cuts from Section ?? leaves an insignificant amount of pure noise events in the sample, the noise simulation is not included in the analysis and won't be listed here.

4.1.1 Expected Rates/Events

The rates and the expected number of events for the SM background are shown in Table 4.1. The explicit detector livetime in the 10 years data taking period is 9.28 years. The rates are calculated by summing the weights of all events in the final level sample, while the uncertainties are calculated by taking the square root of the sum of the weights squared. The expected number of events is calculated by multiplying the rate with the livetime. The individual fractions show that this sample is neutrino dominated where the majority of events are ν_μ -CC events.

add information about the matter profile used

add information about the oscillation probability calculation and the software used for it

Should I adapt the total numbers to match the sum of the rounded individual parts?

Type	Rate [mHz]	Events (in 9.28 years)	Fraction [%]
ν_μ^{CC}	0.3531	103321 ± 113	58.9
ν_e^{CC}	0.1418	41490 ± 69	23.7
ν_{NC}	0.0666	19491 ± 47	11.1
ν_τ^{CC}	0.0345	10094 ± 22	5.8
μ	0.0032	936 ± 15	0.5
total	0.5991	175336 ± 143	100.0

Table 4.1: Final level rates and event expectation of the SM background particle types.

Table 4.2 shows the rates and expected number of events for the HNL signal simulation. The expectation depends on the mass and the mixing and shown here are two example mixings for all the three masses that are being tested in this work. A mixing of 0.0 would result in no HNL events at all. It can already be seen that for the smaller mixing of $|U_{\tau 4}|^2 = 10^{-3}$ the expected number of events is very low, while at the larger mixing of $|U_{\tau 4}|^2 = 10^{-1}$ the number is comparable to the amount of muons in the background sample.

Table 4.2: Final level rates and event expectations of the HNL signal for all three masses and two example mixing values.

HNL mass	Rate [μHz]	Events (in 9.28 years)
$ U_{\tau 4} ^2 = 10^{-1}$		
0.3 GeV	3.3298 ± 0.0053	974.5 ± 1.6
0.6 GeV	3.0583 ± 0.0058	895.0 ± 1.7
1.0 GeV	2.4988 ± 0.0059	731.3 ± 1.7
$ U_{\tau 4} ^2 = 10^{-3}$		
0.3 GeV	0.0057	1.67 ± 0.01
0.6 GeV	0.0220	6.44 ± 0.01
1.0 GeV	0.0248	7.27 ± 0.01

4.1.2 Analysis Binning

[28]: Yu et al. (2023), “Recent neutrino oscillation result with the IceCube experiment”

The identical binning to the analysis performed in [28] is used. It was chosen such that the track-like bin has the largest ν_μ -CC fraction. Extend the binning towards lower energies or increasing the number of bins did not improve the HNL sensitivities significantly. It also has to be considered that sufficient data events need to end up in the individual bins to result in a good fit, which was already investigated in the previous analysis. To mitigate the low data statistics, a few bins were not taken into account in the analysis. There are three bins in PID (cascade-like, mixed and track-like), 12 bins in reconstructed energy, and 8 bins in cosine of the reconstructed zenith angle as specified in Table 4.3. Originally, there were two more bins in $\cos(\theta)$, which were removed to reduce muons coming from the horizon and some low energy bins in the cascade-like bin are removed due to the low event statistics.

add 3D expectation and/or S/\sqrt{B} plots

Add fractions of the different particle types in the bins for benchmark mass/mixing (another table?)

Table 4.3: Three dimensional binning used in the analysis. All variables are from the FLERCNN reconstruction explained in Section ??.

Variable	N_{bins}	Edges	Step
P_ν	3	[0.00, 0.25, 0.55, 1.00]	linear
E	12	[5.00, 100.00]	logarithmic
$\cos(\theta)$	8	[-1.00, 0.04]	linear

4.2 Statistical Analysis

4.2.1 Low Energy Analysis Framework

The analysis is performed using the PISA [29] [30] software framework, which was developed to perform analyses "of small signals in high-statistics neutrino oscillation experiments". It is used to generate the expected event distributions from several MC sets, which can then be compared to the observed data. The expectation for each set is calculated in parallel, applying physics and nuisance parameter effects in a stage-wise manner, before combining the final expectation from all the sets.

[29]: Aartsen et al. (2020), "Computational techniques for the analysis of small signals in high-statistics neutrino oscillation experiments"

4.2.2 Test Statistic

The measurements are performed by comparing the weighted MC to the data. Through variation of the nuisance and physics parameters that govern the weights, the best matching set of parameters can be found. The comparison is done using a modified χ^2 defined as

$$\chi_{\text{mod}}^2 = \sum_{i \in \text{bins}} \frac{(N_i^{\text{exp}} - N_i^{\text{obs}})^2}{N_i^{\text{exp}} + (\sigma_i^{\nu})^2 + (\sigma_i^{\mu})^2 + (\sigma_i^{\text{HNL}})^2} + \sum_{j \in \text{syst}} \frac{(s_j - \hat{s}_j)^2}{\sigma_{s_j}^2}, \quad (4.1)$$

as the *test statistic* (*TS*). The total even expectation is $N_i^{\text{exp}} = N_i^{\nu} + N_i^{\mu} + N_i^{\text{HNL}}$, where N_i^{ν} , N_i^{μ} , and N_i^{HNL} are the expected number of events in bin i from neutrinos, atmospheric muons, and HNLs, while N_i^{obs} is the observed number of events in bin i . The expected number of events from each particle type is calculated by summing the weights of all events in the bin $N_i^{\text{type}} = \sum_i^{\text{type}} \omega_i$, with the statistical uncertainty being $(\sigma_i^{\text{type}})^2 = \sum_i^{\text{type}} \omega_i^2$. The additional term in Equation 4.1 is included to apply a penalty term for prior knowledge of the systematic uncertainties of the parameters where they are known. s_j are the systematic parameters that are varied in the fit, while \hat{s}_j are their nominal values and σ_{s_j} are the known uncertainties.

Do I want/need to include the description of the KDE muon estimation?

4.2.3 Systematic Uncertainties

Add table with all systematic uncertainties used in this analysis (in the analysis chapter).

4.3 Analysis Checks

Fitting to data will be performed in a *blind* manner, where the analyzer does not immediately see the fitted physics and nuisance parameter values, but first checks that a set of pre-defined *goodness of fit* (*GOF*) criteria are fulfilled. If those criteria are met to satisfaction the fit results are unblinded and the full result can be revealed. Before these blind fits to data are run, the robustness of the analysis method is tested using pseudo-data that is generated using the MC sets.

add final level effects of varying the axial mass parameters (or example of one)

add final level effects of varying the DIS parameter (or example of one)

1: There is a degeneracy between the lower octant ($\theta_{23} < 45^\circ$) and the upper octant ($\theta_{23} > 45^\circ$), which can lead to TS minima (local and global) at two positions that are mirrored around 45° in θ_{23} .

[31]: Dembinski et al. (2022), *scikit-hep/iminuit: v2.17.0*

[32]: James et al. (1975), “Minuit: A System for Function Minimization and Analysis of the Parameter Errors and Correlations”

Fit	Err.	Prec.	Tol.
Coarse	1e-1	1e-8	1e-1
Fine	1e-5	1e-14	1e-5

Table 4.4: Migrad settings for the two stages in the minimization routine. *Err.* are the step size for the numerical gradient estimation, *Prec.* is the precision with which the LLH is calculated, and *Tol.* is the tolerance for the minimization.

2: A pseudo-data set without statistical fluctuations is called Asimov data set.

Do I want additional plots for this (fit diff, LLH distr, minim. stats, param. fits)?

Figure 4.1: Asimov inject/recover test for the 0.6 GeV mass set. Mixing values between 10^{-3} and 10^0 are injected and fit back with the full analysis chain. The injected parameter is always recovered within the statistical uncertainty.

4.3.1 Minimization Robustness

To find the set of parameters that describes the data best, a staged minimization routine is used. In the first stage, a fit with coarse minimizer settings is performed to find a rough estimate of the *best fit point (BFP)*. In the second stage, the fit is performed again in both octants¹ of θ_{23} , starting from the BFP of the coarse fit. For each individual fit the *MIGRAD* routine of *iminuit* [31] is used to minimize the χ^2 TS defined in Equation 4.1. *iminuit* is a fast, python compatible minimizer based on the *Minuit2* C++ library [32]. The individual minimizer settings are shown in Table 4.4.

To test the minimization routine and to make sure it consistently recovers any injected physics parameters, pseudo-data sets are produced from the MC by choosing the nominal nuisance parameters and specific physics parameters, without adding any statistical or systematic fluctuations to it. These so-called *Asimov*² data sets are then fit back with the full analysis chain. This type of test is called *Asimov inject/recover test*. A set of mixing values between 10^{-3} and 10^0 is injected and fit back. Even though this range is well within the excluded regions by other experiments, discussed in Section 2.3.3, this covers the current sensitive region of the analysis in IceCube DeepCore. Without fluctuations the fit is expected to always recover the injected parameters (both physics and nuisance parameters). The fitted mixing values from the Asimov inject/recover tests are compared to the true injected values in Figure 4.1 for the 0.6 GeV set. As expected, the fit is always able to recover the injected physics parameter and the nuisance parameters. Additional plots for the other mass sets can be found in Section B.1.



4.3.2 Ensemble Tests

To estimate the goodness of fit, pseudo-data is generated from the MC by injecting the BFP parameters as true parameters and then fluctuating the expected bin counts using Poisson fluctuation. The resulting pseudo-data sets are then fit back with the analysis chain. By comparing the

distribution of TS values from this *ensemble* of pseudo-data trials to the TS of the fit to real data, a p-value can be calculated. The p-value is the probability of finding a TS value at least as large as the one from the data fit. Figure 4.2 shows the TS distribution from the ensemble tests for the 0.6 GeV mass set and the observed TS value from the fit, resulting in a p-value of 28.5 %³. Plots for the addition two mass sets are shown in Section B.1.1.

Add bin-wise TS distribution? Add 3D TS maps?

3: The p-values for the 0.3 GeV and 1.0 GeV are 28.3% and 26.0%, respectively.

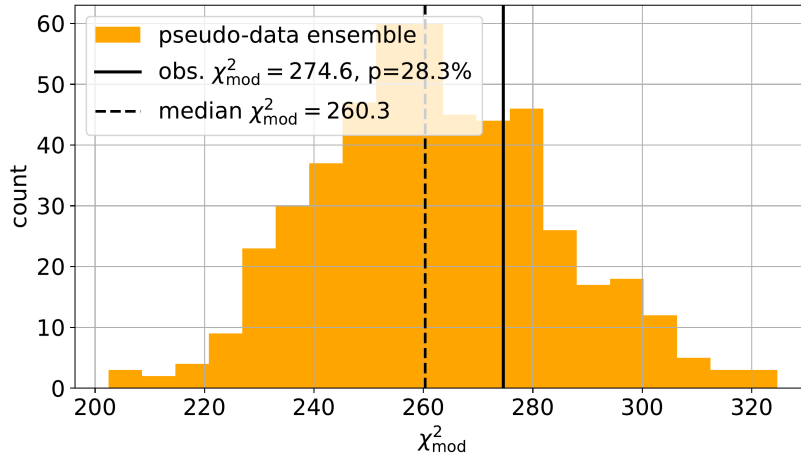


Figure 4.2: Observed fit TS and TS distribution from pseudo-data trials for the 0.6 GeV mass set.

4.4 Results

4.4.1 Best Fit Parameters

4.4.2 Upper Limits

4.4.3 Post-Fit Data/MC Agreement

4.4.4 Likelihood Coverage

APPENDIX

A

Heavy Neutral Lepton Signal Simulation

A.1 Model Independent Simulation Distributions

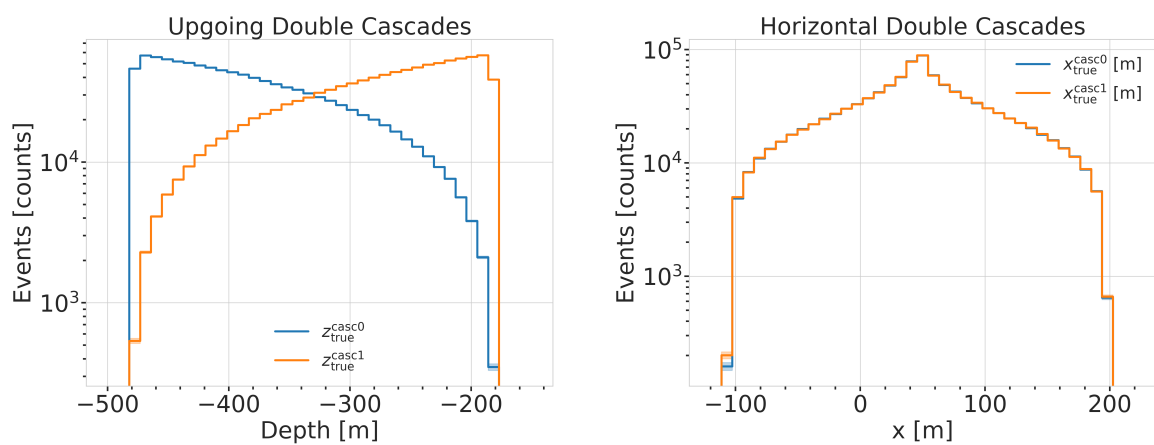


Figure A.1: Generation level distributions of the simplistic simulation sets. Vertical positions (left) and horizontal positions (right) of both sets are shown.

Re-make plot with x,y for horizontal set one plot!

Re-make plot with x, y, z for both cascades in one.

Re-arrange plots in a more sensible way.

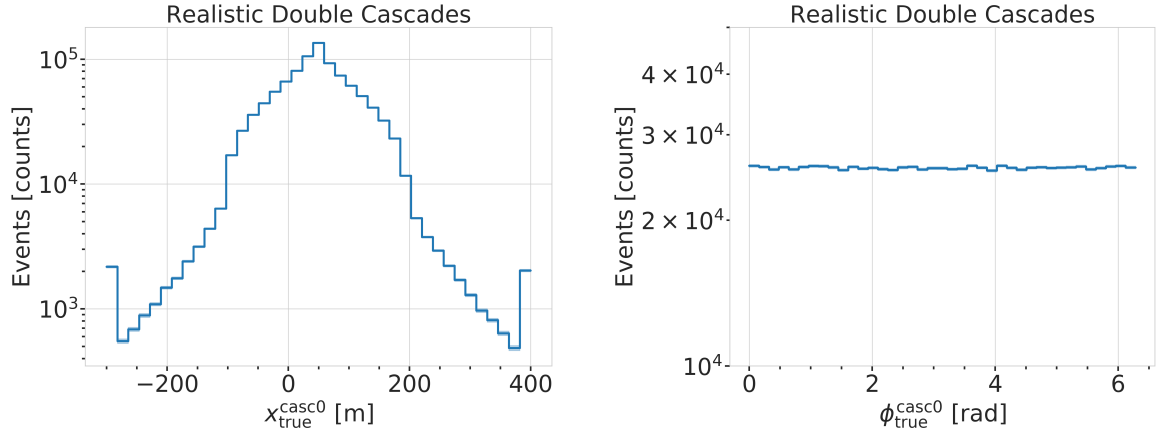


Figure A.2: Generation level distributions of the realistic simulation set. Shown are the cascade x, y, z positions (left) and direction angles (right).

A.2 Model Dependent Simulation Distributions

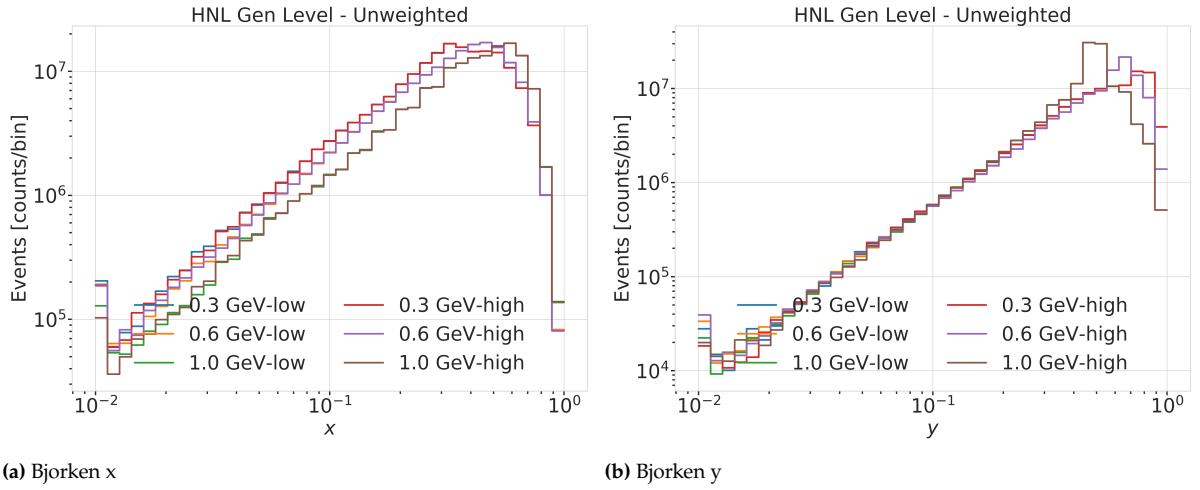


Figure A.3: Generation level distributions of the model dependent simulation.

B

Analysis Checks

B.1 Minimization Robustness

Figure B.1 shows additional Asimov inject/recover tests for the 0.3 GeV and the 1.0 GeV mass sets. The tests were described in Section 4.3.1.

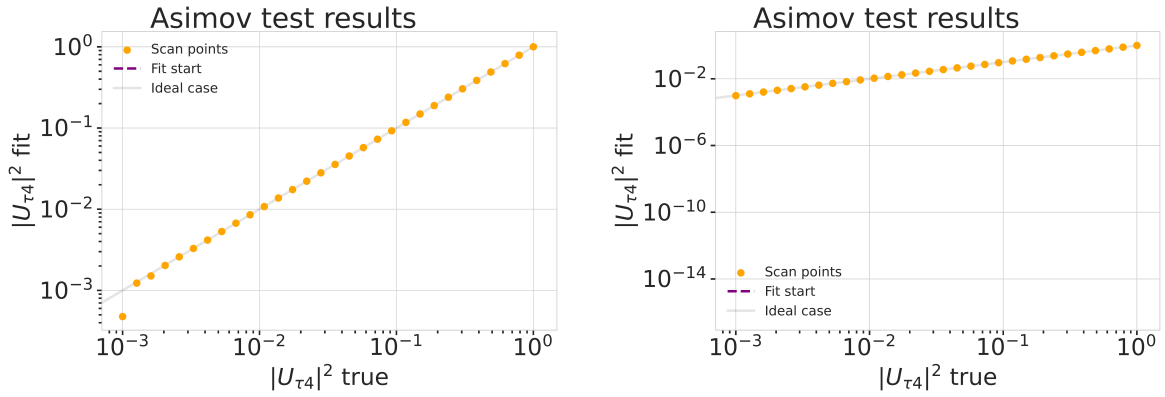


Figure B.1: Asimov inject/recover test for the 0.3 GeV (left) and the 1.0 GeV (right) mass sets. Mixing values between 10^{-3} and 10^0 are injected and fit back with the full analysis chain. The injected parameter is always recovered within the statistical uncertainty.

B.1.1 Ensemble Tests

Figure B.2 shows additional TS distributions from pseudo-data trials and the observed TS from the fit to the data for the ensemble for the 0.3 GeV and the 1.0 GeV mass sets. The tests were described in Section 4.3.2.

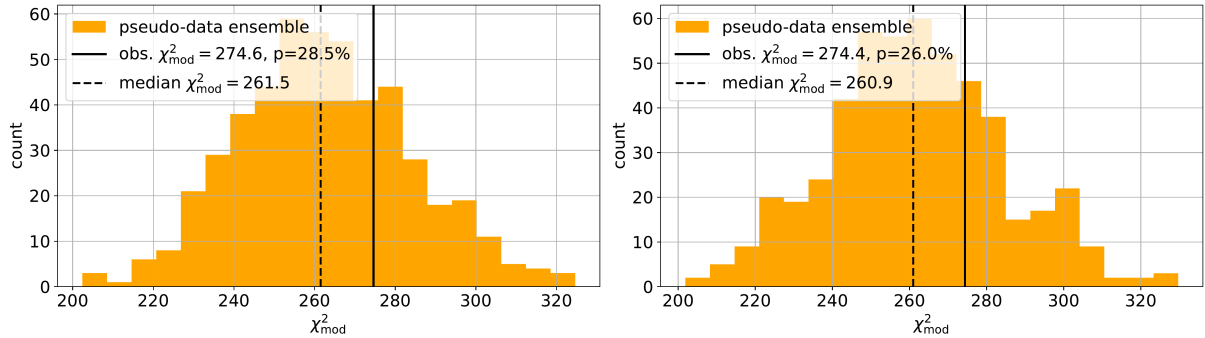


Figure B.2: Observed fit TS and TS distribution from pseudo-data trials for the 0.3 GeV (left) and the 1.0 GeV (right) mass set.

Bibliography

Here are the references in citation order.

- [1] W. Pauli. “Dear radioactive ladies and gentlemen”. In: *Phys. Today* 31N9 (1978), p. 27 (cited on page 1).
- [2] C. L. Cowan et al. “Detection of the Free Neutrino: a Confirmation”. In: *Science* 124.3212 (1956), pp. 103–104. doi: [10.1126/science.124.3212.103](https://doi.org/10.1126/science.124.3212.103) (cited on page 1).
- [3] G. Danby et al. “Observation of High-Energy Neutrino Reactions and the Existence of Two Kinds of Neutrinos”. In: *Phys. Rev. Lett.* 9 (1 July 1962), pp. 36–44. doi: [10.1103/PhysRevLett.9.36](https://doi.org/10.1103/PhysRevLett.9.36) (cited on page 1).
- [4] K. Kodama et al. “Observation of tau neutrino interactions”. In: *Physics Letters B* 504.3 (2001), pp. 218–224. doi: [https://doi.org/10.1016/S0370-2693\(01\)00307-0](https://doi.org/10.1016/S0370-2693(01)00307-0) (cited on page 1).
- [5] R. Davis et al. *Proceedings of the Neutrino '72 Europhysics Conference*. Vol. 1. Baltonfuered, Hungary, 1972, p. 29 (cited on page 1).
- [6] M. G. Aartsen et al. “The IceCube Neutrino Observatory: instrumentation and online systems”. In: *Journal of Instrumentation* 12.3 (Mar. 2017), P03012. doi: [10.1088/1748-0221/12/03/P03012](https://doi.org/10.1088/1748-0221/12/03/P03012) (cited on page 1).
- [7] C. Giunti and C. W. Kim. *Fundamentals of Neutrino Physics and Astrophysics*. Oxford University Press, Mar. 2007 (cited on page 3).
- [8] M. D. Schwartz. *Quantum Field Theory and the Standard Model*. Cambridge University Press, 2013 (cited on page 3).
- [9] T. Yanagida. “Horizontal Symmetry and Masses of Neutrinos”. In: *Progress of Theoretical Physics* 64.3 (Sept. 1980), pp. 1103–1105. doi: [PTP.64.1103](https://doi.org/10.1093/ptp/64.3.1103) (cited on page 4).
- [10] P. Astier et al. “Search for heavy neutrinos mixing with tau neutrinos”. In: *Phys. Lett. B* 506 (2001), pp. 27–38. doi: [10.1016/S0370-2693\(01\)00362-8](https://doi.org/10.1016/S0370-2693(01)00362-8) (cited on page 5).
- [11] R. Acciarri et al. “New Constraints on Tau-Coupled Heavy Neutral Leptons with Masses $m_N=280\text{--}970$ MeV”. In: *Phys. Rev. Lett.* 127.12 (2021), p. 121801. doi: [10.1103/PhysRevLett.127.121801](https://doi.org/10.1103/PhysRevLett.127.121801) (cited on page 5).
- [12] J. Orloff, A. N. Rozanov, and C. Santoni. “Limits on the mixing of tau neutrino to heavy neutrinos”. In: *Phys. Lett. B* 550 (2002), pp. 8–15. doi: [10.1016/S0370-2693\(02\)02769-7](https://doi.org/10.1016/S0370-2693(02)02769-7) (cited on page 5).
- [13] I. Boiarska et al. “Blast from the past: constraints from the CHARM experiment on Heavy Neutral Leptons with tau mixing”. In: (July 2021) (cited on page 5).
- [14] P. Abreu et al. “Search for neutral heavy leptons produced in Z decays”. In: *Z. Phys. C* 74 (1997). [Erratum: *Z.Phys.C* 75, 580 (1997)], pp. 57–71. doi: [10.1007/s002880050370](https://doi.org/10.1007/s002880050370) (cited on page 5).
- [15] P. Coloma et al. “Double-Cascade Events from New Physics in Icecube”. In: *Phys. Rev. Lett.* 119.20 (2017), p. 201804. doi: [10.1103/PhysRevLett.119.201804](https://doi.org/10.1103/PhysRevLett.119.201804) (cited on pages 4, 5).
- [16] P. Coloma. “Icecube/DeepCore tests for novel explanations of the MiniBooNE anomaly”. In: *Eur. Phys. J. C* 79.9 (2019), p. 748. doi: [10.1140/epjc/s10052-019-7256-8](https://doi.org/10.1140/epjc/s10052-019-7256-8) (cited on page 5).
- [17] P. Coloma et al. “GeV-scale neutrinos: interactions with mesons and DUNE sensitivity”. In: *Eur. Phys. J. C* 81.1 (2021), p. 78. doi: [10.1140/epjc/s10052-021-08861-y](https://doi.org/10.1140/epjc/s10052-021-08861-y) (cited on pages 6, 8).
- [18] M. Thomson. *Modern particle physics*. Cambridge [u.a.]: Cambridge University Press, 2013, XVI, 554 S. (Cited on page 9).
- [19] S. L. Glashow. “Partial-symmetries of weak interactions”. In: *Nuclear Physics* 22.4 (1961), pp. 579–588. doi: [https://doi.org/10.1016/0029-5582\(61\)90469-2](https://doi.org/10.1016/0029-5582(61)90469-2) (cited on page 9).
- [20] M. Tanabashi et al. “Review of Particle Physics”. In: *Phys. Rev. D* 98 (3 Aug. 2018), p. 030001. doi: [10.1103/PhysRevD.98.030001](https://doi.org/10.1103/PhysRevD.98.030001) (cited on pages 9, 11, 12).

- [21] A. Terliuk. “Measurement of atmospheric neutrino oscillations and search for sterile neutrino mixing with IceCube DeepCore”. PhD thesis. Berlin, Germany: Humboldt-Universität zu Berlin, Mathematisch-Naturwissenschaftliche Fakultät, 2018. doi: [10.18452/19304](https://doi.org/10.18452/19304) (cited on pages 9, 11).
- [22] J. A. Formaggio and G. P. Zeller. “From eV to EeV: Neutrino cross sections across energy scales”. In: *Rev. Mod. Phys.* 84 (3 Sept. 2012), pp. 1307–1341. doi: [10.1103/RevModPhys.84.1307](https://doi.org/10.1103/RevModPhys.84.1307) (cited on page 10).
- [23] M. Honda et al. “Atmospheric neutrino flux calculation using the NRLMSISE-00 atmospheric model”. In: *Phys. Rev. D* 92 (2 July 2015), p. 023004. doi: [10.1103/PhysRevD.92.023004](https://doi.org/10.1103/PhysRevD.92.023004) (cited on page 11).
- [24] A. Fedynitch et al. “Calculation of conventional and prompt lepton fluxes at very high energy”. In: *European Physical Journal Web of Conferences*. Vol. 99. European Physical Journal Web of Conferences. Aug. 2015, p. 08001. doi: [10.1051/epjconf/20159908001](https://doi.org/10.1051/epjconf/20159908001) (cited on page 12).
- [25] M. Honda et al. “Calculation of atmospheric neutrino flux using the interaction model calibrated with atmospheric muon data”. In: *Phys. Rev. D* 75 (4 Feb. 2007), p. 043006. doi: [10.1103/PhysRevD.75.043006](https://doi.org/10.1103/PhysRevD.75.043006) (cited on page 12).
- [26] S. Bilenky and B. Pontecorvo. “Lepton mixing and neutrino oscillations”. In: *Physics Reports* 41.4 (1978), pp. 225–261. doi: [10.1016/0370-1573\(78\)90095-9](https://doi.org/10.1016/0370-1573(78)90095-9) (cited on page 12).
- [27] P. A. M. Dirac. “The Quantum Theory of the Emission and Absorption of Radiation”. In: *Proceedings of the Royal Society of London Series A* 114.767 (Mar. 1927), pp. 243–265. doi: [10.1098/rspa.1927.0039](https://doi.org/10.1098/rspa.1927.0039) (cited on page 12).
- [28] S. Yu and J. Micallef. “Recent neutrino oscillation result with the IceCube experiment”. In: *38th International Cosmic Ray Conference*. July 2023 (cited on page 18).
- [29] M. G. Aartsen et al. “Computational techniques for the analysis of small signals in high-statistics neutrino oscillation experiments”. In: *Nucl. Instrum. Meth. A* 977 (2020), p. 164332. doi: [10.1016/j.nima.2020.164332](https://doi.org/10.1016/j.nima.2020.164332) (cited on page 19).
- [30] I. Collaboration. <https://github.com/icecube/pisa> (cited on page 19).
- [31] H. Dembinski et al. *scikit-hep/iminuit: v2.17.0*. Version v2.17.0. Sept. 2022. doi: [10.5281/zenodo.7115916](https://doi.org/10.5281/zenodo.7115916) (cited on page 20).
- [32] F. James and M. Roos. “Minuit: A System for Function Minimization and Analysis of the Parameter Errors and Correlations”. In: *Comput. Phys. Commun.* 10 (1975), pp. 343–367. doi: [10.1016/0010-4655\(75\)90039-9](https://doi.org/10.1016/0010-4655(75)90039-9) (cited on page 20).